

Chapter 1

Baryons and Chiral Symmetry

Keh-Fei Liu *

*Dept. of Physics and Astronomy, University of Kentucky
Lexington, KY 40506 USA*

The relevance of chiral symmetry in baryons is highlighted in three examples in the nucleon spectroscopy and structure. The first one is the importance of chiral dynamics in understanding the Roper resonance. The second one is the role of chiral symmetry in the lattice calculation of $\pi N\sigma$ term and strangeness. The third one is the role of chiral $U(1)$ anomaly in the anomalous Ward identity in evaluating the quark spin and the quark orbital angular momentum. Finally, the chiral effective theory for baryons is discussed.

1. Introduction

It is well-known that for three-flavor Quantum Chromodynamics (QCD), the chiral symmetry $SU(3)_L \times SU(3)_R$ is spontaneously broken to the diagonal $SU(3)_V$ with the octet pseudoscalar mesons as the Goldstone boson. There is also a $U_A(1)$ anomaly which begets a heavy η' meson. As such, pions and chiral symmetry are important for low-energy hadron physics and the chiral dynamics has been successfully applied in subjects such as $\pi\pi$ scattering,^{1,2} vector dominance,³ KSFR relation,⁴ low-energy πN scatterings,^{1,5} πN scattering up to about 1 GeV with the skyrmion,⁶ nucleon static properties,⁷ electromagnetic form factors,⁷ πNN form factor,⁸ and the Goldberger-Treiman relation.⁹

The long range part of the nucleon-nucleon potential is due to one pion exchange and more modern NN potential has included the correlated two-pion exchange potential to account for the intermediate range attraction.^{10,11} These are the major ingredients in the realistic phase-shift equivalent NN potentials.¹²

*liu@pa.uky.edu

Realization and application of chiral symmetry in hadrons and nuclei has been a major research theme in Gerry Brown's scientific career. These include chiral symmetry in nucleon-nucleon interaction,¹³ meson exchange currents,¹⁴ and his joint research effort with Mannque Rho on little chiral bag,¹⁵ Brown-Rho scaling,¹⁶ and dense nuclear matter.¹⁷

With the advent of Quantum Chromodynamics (QCD) and the lattice chiral fermion formulations in domain wall fermion¹⁸ and overlap fermion,¹⁹ lattice QCD has provided a new tool in addressing the role of chiral symmetry and the associated dynamics in first principle's calculation in terms of quarks and gluons.

In this memorial manuscript, I will discuss 3 examples in baryons where chiral symmetry plays a crucial role as a way to pay tribute to Gerry's teaching throughout the author's professional career and to echo his passion of chiral symmetry by extending the study of chiral symmetry from nuclear structure to nucleon structure.²⁰

The 3 examples are the Roper resonance, the pion nucleon sigma term and strangeness, and the quark spin as representative cases for the importance of chiral symmetry in baryon spectroscopy and structure.

2. Roper resonance

The Roper resonance has been studied extensively, but its status as the lowest excited state of the nucleon with the same quantum numbers is intriguing. First of all, it has been noted for a long time that it is rather unusual to have the first positive parity excited state lower than the negative parity excited state which is the $N_{1/2}^-(1535)$ in the S_{11} πN scattering channel. This is contrary to the excitation pattern in the meson sectors with either light or heavy quarks. This parity reversal has been problematic for the quark models based on $SU(6)$ symmetry with color-spin interaction between the quarks²¹ which cannot accommodate such a pattern. Realistic potential calculations with linear and Coulomb potentials²² and the relativistic quark model²³ all predict the Roper to be $\sim 100 - 200$ MeV above the experimental value with the negative parity state lying lower. On the other hand, the pattern of parity reversal was readily obtained in the chiral soliton model like the Skyrme model via the small oscillation approximation to πN scattering.⁶ Although the first calculation²⁴ of the original skyrmion gives rise to a breathing mode which is ~ 200 MeV lower than the Roper resonance, it was shown later²⁵ that the introduction of the sixth order term, which is the zero range approximation for the ω meson coupling,

changes the compression modulus and produces a better agreement with experiment for both the mass and width in πN scattering.

Since the quark potential model is based on the $SU(6)$ symmetry with residual color-spin interaction between the quarks; whereas, the chiral soliton model is based on spontaneous broken chiral symmetry, their distinctly different predictions on the ordering of the positive and negative parity excited states may well be a reflection of different dynamics as a direct consequence of the respective symmetry. This possibility has prompted Glozman and Riska to suggest²⁶ that the parity reversal in the excited nucleon and Δ , in contrast to that in the excited Λ spectrum, is an indication that the inter-quark interaction of the light quarks is mainly of the flavor-spin nature, which implies Goldstone boson exchange, rather than the color-spin nature due to the one-gluon exchange. This suggestion is supported in the lattice QCD study of "Valence QCD"²⁷ where one finds that the hyperfine splitting between the nucleon and Δ and also between ρ and π are largely decimated when the Z -graphs in the quark propagators are removed. This is an indication that the color-magnetic interaction is not the primary source of the inter-quark spin-spin interaction for light quarks. (The color-magnetic part, being spatial in origin, should be unaffected by the truncation of Z -graphs in Valence QCD, which only affects the time part.) Yet, it is consistent with the Goldstone-boson-exchange picture which requires Z -graphs and thus the flavor-spin interaction.

The failure of the $SU(6)$ quark model to delineate the Roper and its photo-production has prompted the speculation that the Roper resonance may be a hybrid state with excited glue²⁸ or a $qqqq\bar{q}$ five quark state.²⁹ Thus, unraveling the nature of Roper resonance has direct bearing on our understanding of the quark structure and chiral dynamics of baryons.

Lattice QCD is, in principle, the most desirable tool to adjudicate the theoretical controversy surrounding the issue. However, there is a complication. As shown in Fig. 2, the lattice calculations with the Clover fermions,^{30–32} chirally improved fermions,³³ and twisted mass fermions³² agree with the overlap fermion for the nucleon mass,³⁴ but their first excited nucleon state (i.e. the Roper) are mostly over 2 GeV and much higher than those of the overlap fermion in the pion mass range between 300 MeV and 600 MeV. Near the physical pion mass, they are ~ 300 MeV above the experimental Roper mass at ~ 1430 MeV, while the overlap fermion prediction agrees with experiment. This situation is basically a redux of the quenched calculations,^{35,36} i.e. the overlap results are much lower than those of the Wilson type fermions. Why is there such a discrepancy? Since

the calculations with Wilson type fermions, which breaks chiral symmetry, use the variational calculation, while the calculation with the chiral overlap fermion adopts the Sequential Empirical Bayes Method (SEB)³⁷ to extract the Roper state, a question arises as to whether the discrepancy is due to different fitting algorithms or different actions at finite lattice spacing.

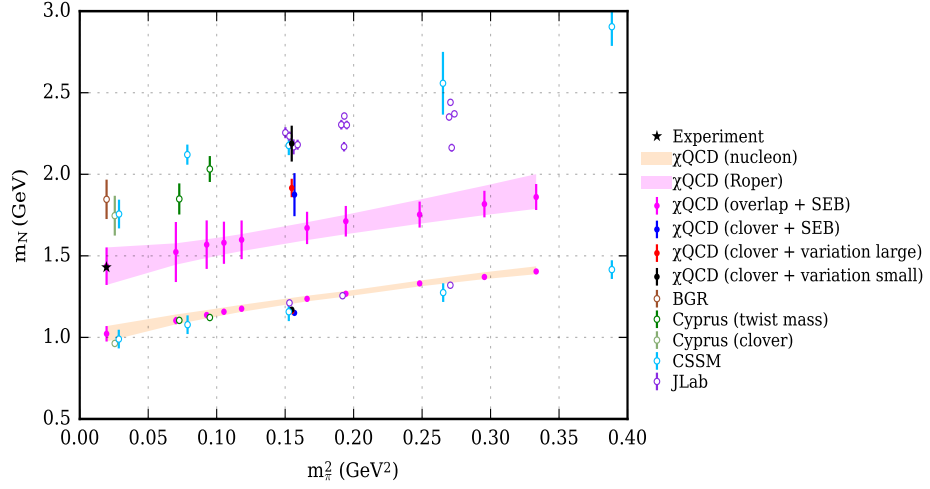


Fig. 1. Comparison of nucleon and Roper masses as a function of m_π^2 in several dynamical fermion calculations with different fermion actions.

It was previously reported³⁴ that to check the different algorithmic approaches, the SEB method was used on the gauge configurations that are produced by HSC Collaboration³¹ to calculate the nucleon and the Roper. These are 2+1 flavor Clover fermion gauge configurations on the anisotropic $24^3 \times 128$ lattice with $a_s = 0.123$ fm and the light u/d sea quark mass corresponds to a pion mass of ~ 390 MeV (*N.B.* the HSC results in Fig. 1 were obtained on the $16^3 \times 128$ lattice with the same action and quark mass.) The SEB fitting of the nucleon and Roper masses are shown in Fig. 1 together with the variational results from HSC.³¹ We see that while the nucleon mass agrees with that from HSC; the Roper, on the other hand, is lower than that from HSC by ~ 300 MeV (blue point in Fig. 1) with a $\sim 3\sigma$ difference. To verify that this difference is not due to the fitting algorithm, we have carried out a variational calculation with different smearing sizes for the interpolation field. We see that when the r.m.s. radii of the Gaussian smeared source include one as large as 0.86 fm, the Roper does ap-

pear lower at 1.92(6) GeV as shown by the second plateau in Fig. 2 (upper panel) and indicated by the red point in Fig. 1. This is in agreement with the SEB result which is shown as the blue point in Fig. 1. On the other hand, when the r.m.s. radii of all the Gaussian smeared sources are less than 0.4 fm, the nucleon excited state is higher – 2.19(11) GeV as shown in Fig. 2 (lower panel) and indicated by the black dot in Fig. 1, which is consistent with the HSC result indicated by the purple points in the same figure. This presumably confirms the speculation³⁴ that one needs a large enough source to have a better overlap with the 2S excited state which has a radial node at ~ 0.9 fm from the study of its Coulomb wavefunction;³⁴ whereas, smaller sources may couple to the 3S state strongly and results in a higher mass. More importantly, the fact that this new variational result agrees with that from the SEB method suggests that the SEB method is a legitimate approach and, consequently, its extraction of the Roper at ~ 1.6 GeV in this pion mass range from the overlap fermion calculation in Fig. 1 should be reliable.

The fitting algorithm issue being settled, this leads to the possibility that the difference is due to the different fermion actions at finite lattice spacing.

An extensive model has been constructed to study the N^* resonance in πN scattering partial waves.³⁸ The unperturbed states are the bare N and Δ and the meson-baryon reaction channels including πN , ηN , and $\pi\pi N$ which has $\pi\Delta$, ρN , and σN resonant components. This model fits the πN scattering data well in various channels below 2 GeV. It is found³⁹ in the P_{11} channel, the meson-baryon transition amplitude is strong, which shifts the bare $1/2^+ N^*$ at 1763 MeV down to $(\text{Re}M_R, -\text{Im}M_R) = (1357, 76)$ MeV which corresponds to the P_{11} pole of $N^*(1440)$. This is a shift of ~ 400 MeV in mass due to the meson-baryon coupling. Compared to the overlap fermion which has the lattice chiral symmetry which can have a larger $\langle 0 | \chi_{N,3q} | \pi N \rangle$ matrix element and a large Roper to πN coupling. These 3 quark to 5 quark coupling which invokes a pair creation or the Z-graph might be curtailed in the Wilson fermions like in “Valence QCD” as we discussed above and consequently results in a higher Roper state. This is a plausible explanation which is verifiable with variational calculations of the Roper state with the Wilson-Clover fermion at smaller lattice spacings where chiral symmetry is better recovered. Given the pattern of level reversal, the πN scattering model and the lattice calculations, we believe the Roper resonance has a sizable πN component in its wavefunction³⁴ and is a showcase for the role of chiral dynamics.

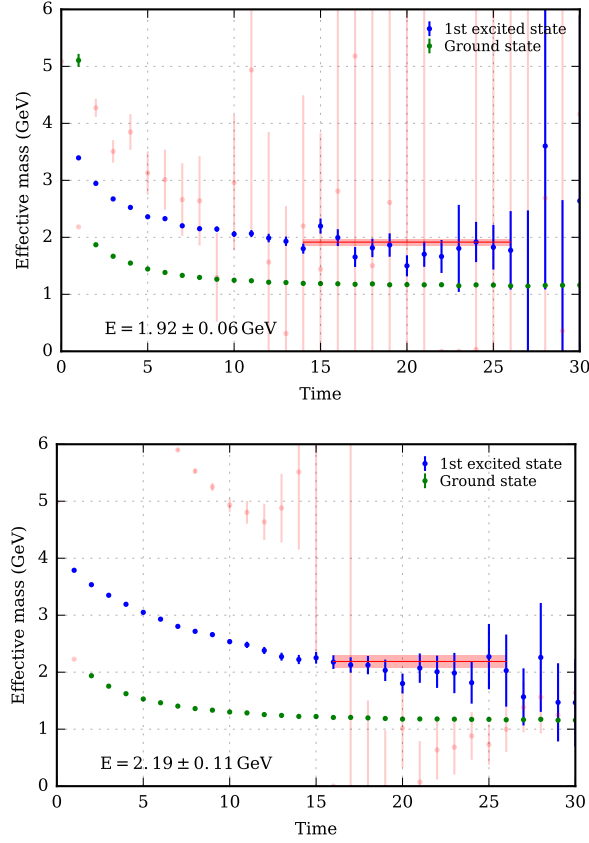


Fig. 2. Nucleon and Roper masses from the variational method including large smeared sources with radius as large as 0.86 fm (upper panel) and with the radius of the smeared sources limited to less than 0.4 fm (lower panel).

3. πN and strangeness sigma terms

As measures of explicit and spontaneous chiral symmetry breaking in the baryon sector, $\sigma_{\pi N}$, defined as

$$\sigma_{\pi N} \equiv \hat{m} \langle N | \bar{u}u + \bar{d}d | N \rangle, \quad (1)$$

where $\hat{m} = (m_u + m_d)/2$ is the averaged light quark mass, and f_s^N defined as the strangeness σ term as a fraction of the nucleon mass

$$\sigma_{sN} \equiv m_s \langle N | \bar{s}s | N \rangle, \quad f_s^N = \frac{\sigma_{sN}}{m_N}, \quad (2)$$

are fundamental quantities which pertain to a wide range of issues in hadron physics. They include the quark mass contribution in the baryon which is

related to the Higgs contribution to the observable matter,^{40,41} the pattern of SU(3) breaking,⁴⁰ πN and KN scatterings,^{42,43} and kaon condensate in dense matter.⁴⁴ Using the sum rule of the nucleon mass, the heavy quark mass contribution can be deduced by that from the light favors, in the heavy quark limit and also in the leading order of the coupling.^{41,45,46} At the same time, precise values of the quark mass term for various flavors, from light to heavy, are of high interest for dark matter searches,^{47–49} where the popular candidate of dark matter (likes the weakly interacting mass particle) interacts with the observable world throughout the Higgs couplings, so that the precise determination of the $\sigma_{\pi N}$ and σ_{sN} can provide constraints on the dark matter candidates.

Phenomenologically, the $\sigma_{\pi N}$ term is typically extracted from the πN scattering amplitude. To lowest order in m_π^2 , the unphysical on-shell isospin-even πN scattering amplitude at the Cheng-Dashen point corresponds to $\sigma(q^2 = 2m_\pi^2)$ ^{42,43} which can be determined from πN scattering via fixed- q^2 dispersion relation.⁴³ $\sigma_{\pi N}$ at $q^2 = 0$ can be extracted through a soft correlated two-pion form factor.^{50–52} Analysis of the πN scattering amplitude to obtain $\sigma_{\pi N}(0)$ from the Lorentz covariant baryon chiral perturbation and the Cheng-Dashen low-energy theorem are also developed.^{53–55} They give $\sigma_{\pi N}$ values in the range $\sim 45 - 64$ MeV, while the most recent analysis⁵⁵ gives 59.1(3.5) MeV.

Lattice calculations should be a good tool in giving reliable results to these quantities. Again, there is an issue about chiral symmetry. It was pointed out^{56,57} that due to explicit chiral symmetry breaking, the quark mass in the Wilson type fermions has an additive renormalization and the flavor-singlet and non-singlet quark masses renormalize differently. In this case, the renormalized strange scalar matrix element $\langle N | \bar{s}s | N \rangle^R$ can be written as

$$\langle N | \bar{s}s | N \rangle^R = \frac{1}{3} \left[(Z_0 + 2Z_8) \langle N | \bar{s}s | N \rangle + (Z_0 - Z_8) \langle N | \bar{u}u + \bar{d}d | N \rangle \right], \quad (3)$$

where Z_0 and Z_8 are the flavor-singlet and flavor-octet renormalization constants respectively. Z_0 differs from Z_8 by a disconnected diagram which involves a quark loop. In the massless renormalization scheme, one can calculate these renormalization constants perturbatively. For the massless case where $\bar{\psi}\psi = \bar{\psi}_L\psi_R + \bar{\psi}_R\psi_L$, a quark loop for the scalar density vanishes no matter how many gluon insertions there are on the loop, since the coupling involving γ_μ does not change helicity. Thus, the massless scalar quark loop is zero and $Z_0 = Z_8$. There is no mixing of the scalar matrix element with that of u and d . This is the same with the overlap fermion, since the overlap

has chiral symmetry and the inverse of its massless quark propagator D_c anti-commutes with γ_5 , i.e. $\{D_c, \gamma_5\} = 0$ as in the continuum.

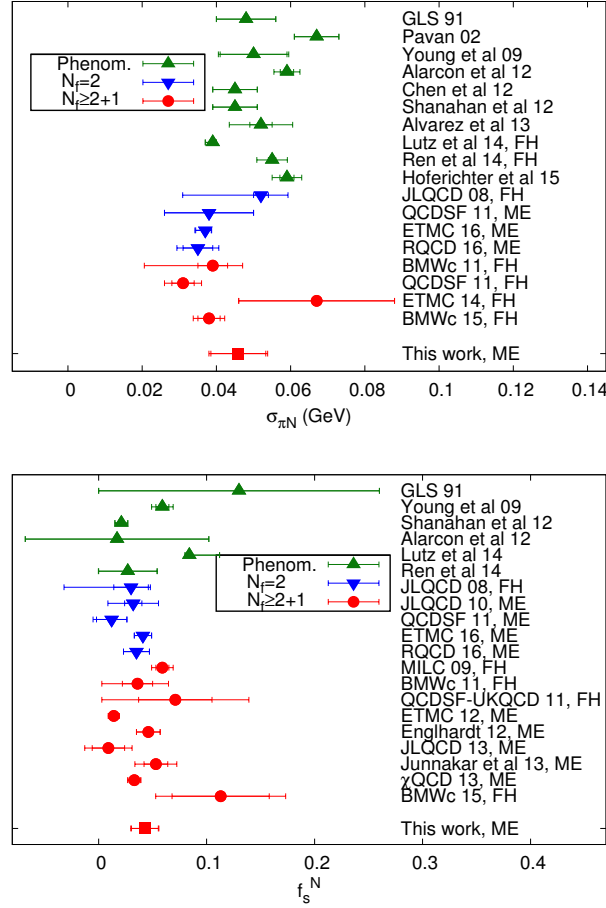


Fig. 3. The results of $\sigma_{\pi N}$ (upper panel) and f_s^N (lower panel) from both phenomenology and lattice simulations. The narrow error bar for each data point is the statistical, and the broad one is that for the total uncertainty. The physical proton mass 938MeV is used to obtain f_s^N in this work. They are color-coded in phenomenological and indirect approaches (green), $N_f = 2$ lattice calculations (blue), and $N_f = 2 + 1$ lattice calculations (red). Detailed references are given in Ref.⁵⁹

This is not so for Wilson type fermion where its free quark propagator contains a term proportional to the Wilson r term which violates chiral

symmetry and will give a non-zero contribution to the scalar matrix element at the massless limit, leading to $Z_0 \neq Z_8$. Since the u and d matrix elements in the nucleon are not small, there can be a substantial flavor mixing at finite a . This lattice artifact due to non-chiral fermions can be removed by calculating Z_0 and Z_8 .⁵⁸ Furthermore, the direct calculation of the matrix element with Wilson type fermions faces the complication that the sigma term with bare quark mass is not renormalization group invariant. This can also be corrected with the introduction of various renormalization constants to satisfy the Ward identities.⁵⁸ All of these involve additional work and will introduce additional errors. On the contrary, there is no flavor mixing in the overlap fermion and the sigma terms are renormalization group invariant with bare mass and bare matrix element, since the renormalization constants of quark mass and scalar operator cancel, i.e. $Z_m Z_s = 1$ due to chiral symmetry. For the latest calculation with overlap fermion on $2 + 1$ flavor domain wall fermion gauge configurations for several ensembles with different lattice spacings, volume, and sea masses including one at the physical pion mass, the global fit gives the prediction of $\sigma_{\pi N} = 45.9(7.4)(2.8)$ MeV and $\sigma_{sN} = 40.2(11.7)(3.5)$ MeV. This value of $\sigma_{\pi N}$ has a two-sigma tension with the recent results based on Roy-Steiner equations⁵⁵ which gives $\sigma_{\pi N} = 59.1(3.5)$ MeV.

To conclude, we believe that to calculate $\sigma_{\pi N}$ and σ_{sN} which are fundamental quantities reflecting both the explicit and spontaneous chiral symmetry, it is theoretically clean and straightforward procedure-wise to calculate them with chiral fermions on the lattice in order to obtain reliable results without the complication of renormalization and flavor-mixing as compared to non-chiral fermions.

4. Quark spin and orbital angular momentum

The quark spin content of the nucleon was found to be much smaller than that expected from the quark model by the polarized deep inelastic lepton-nucleon scattering experiments and the recent global analysis reveals that the total quark spin contributes only $\sim 25\%$ to the proton spin.⁶⁰ This is dubbed 'proton spin crisis' since no model seems to be able to explain it convincingly and, moreover, quantitatively.

Once again, first principle lattice calculation should be able to address this issue. The ideal calculation would be to use the conserved axial-vector current of the chiral fermions which satisfies the anomalous Ward identity (AWI) on lattice at finite lattice spacing. However, it is somewhat involved

to construct the current itself for the overlap fermion.⁶¹ Before it is implemented, one can use the AWI as the normalization condition for the simpler local axial-vector current

$$\partial_\mu \kappa_A A_\mu^1 = 2mP - 2iN_f q, \quad (4)$$

where $A_\mu^1 = \sum_{i=u,d,s} \bar{\psi}_i i\gamma_\mu \gamma_5 (1 - \frac{1}{2} D_{ov}) \psi_i$ is the local singlet axial-vector current and $mP = \sum_{i=u,d,s} m_i \bar{\psi}_i i\gamma_5 (1 - \frac{1}{2} D_{ov}) \psi_i$ is the pseudoscalar density with D_{ov} being the massless overlap operator and q the local topological charge as derived in the Jacobian factor from the fermion determinant under the chiral transformation whose local version is equal to $\frac{1}{16\pi^2} \text{tr}_c G_{\mu\nu} \tilde{G}_{\mu\nu}(x)$ in the continuum,⁶² i.e.

$$q(x) = \text{Tr} \gamma_5 \left(\frac{1}{2} D_{ov}(x, x) - 1 \right) \xrightarrow{a \rightarrow 0} \frac{1}{16\pi^2} \text{tr}_c G_{\mu\nu} \tilde{G}_{\mu\nu}(x). \quad (5)$$

κ_A in Eq. (4) is the finite lattice renormalization factor (often referred to as Z_A in the literature for the flavor non-singlet case) needed for the local axial-vector current to satisfy the AWI on the lattice with finite lattice spacing, much like the finite renormalization for the vector and non-singlet axial-vector currents. We shall call it lattice normalization. On the other hand, the mP and q defined with the overlap operators do not have multiplicative renormalization. There is a two-loop renormalization of the singlet A_μ^1 and the topological charge q mixes with $\partial_\mu A_\mu^1$. It turns out that they are the same. Thus, the renormalized AWI is the same as the unrenormalized AWI (but normalized) to the α_s^2 order. To utilize the AWI, one needs to calculate the matrix elements of $2mP$ and $2q$ on the r.h.s. of the AWI and extrapolate to $q^2 = 0$. However, the smallest $|q^2|$ is larger than the pion mass squared on the lattices that we work on, the extrapolation to q^2 is not reliable. Instead, we shall match the form factors at finite $|q^2|$ from both sides, i.e.

$$2m_N \kappa_A g_A^1(q^2) + q^2 \kappa_A h_A^1(q^2) = 2m g_P(q^2) + N_f g_G(q^2). \quad (6)$$

where the singlet $g_A^1(q^2)$ and the induced pseudoscalar $h_A^1(q^2)$ are the bare form factors. $2m g_P(q^2)$ and $g_G(q)$ are the form factors for the pseudoscalar current and topology respectively. From this normalization condition one can determine κ_A and the normalized g_A^1 is $\kappa_A g_A^1(0)$. This has been employed in the calculation of the strange quark spin to find $\Delta s + \Delta \bar{s} = -0.0403(44)(61)$.⁶³ This is more negative than the other lattice calculations with and axial-vector current, mainly because $\kappa_A = 1.36(4)$ is found to be larger than that of the flavor-octet axial-vector current. The lesson here is that, unless the conserved current is used to carry out the

calculation, it is essential to adopt the AWI to obtain the normalization of the local axial-vector current. This is possible with the overlap fermion.

While the final numbers on the u and d spin fraction which include the connected insertion are still being worked out, the initial results indicate that it is the larger negative $2mP$ matrix elements that cancel the positive topological charge term in the triangle anomaly in the disconnected insertions that lead to a small g_A^1 .

There are various ways to decompose the proton spin into quark and glue spins and orbital angular momenta.^{64,65} From the symmetrized energy-momentum tensor of QCD (the Belinfante form), it is shown⁶⁶ that the proton spin can be decomposed as

$$\vec{J}_{\text{QCD}} = \vec{J}_q + \vec{J}_g = \frac{1}{2}\vec{\Sigma}_q + \vec{L}_q + \vec{J}_g, \quad (7)$$

where the quark angular momentum \vec{J}_q is the sum of quark spin and orbital angular momentum,

$$\vec{J}_q = \frac{1}{2}\vec{\Sigma}_q + \vec{L}_q = \int d^3x \left[\frac{1}{2} \bar{\psi} \vec{\gamma} \gamma^5 \psi + \psi^\dagger \{ \vec{x} \times (i\vec{D}) \} \psi \right], \quad (8)$$

and each of which is gauge invariant. The glue angular momentum operator

$$\vec{J}_g = \int d^3x \left[\vec{x} \times (\vec{E} \times \vec{B}) \right], \quad (9)$$

is also gauge invariant. However, it cannot be further divided into the glue spin and orbital angular momentum gauge invariantly with the Belinfante tensor.

Since it has a large finite volume effect to calculate the operator with a spatial \vec{r} on the lattice with periodic boundary condition, one can instead calculate the quark and glue momentum and angular momentum from their form factors $T_1(q^2)$ and $T_2(q^2)$ and obtain the momentum and angular momentum fractions from their forward limits, i.e. $\langle x \rangle = T_1(0)$ and $J = \frac{1}{2}(T_1(0) + T_2(0))$, much like the electric charge and magnetic moment from the forward Dirac and Pauli form factors $F_1(0)$ and $F_2(0)$. After determining the quark angular momentum, the quark orbital angular momentum is obtained by subtracting the quark spin from it. This has been carried out in a quenched approximation.⁶⁷ The OAM fractions $2\langle L_{\text{kin}}^q \rangle$ for the u and d quarks in the CI have different signs and add up to 0.01(10), i.e. essentially zero. This is the same pattern which has been seen with dynamical fermion configurations and light quarks, as pointed out earlier. The large OAM fractions $2\langle L_{\text{kin}}^q \rangle$ for the u/d and s quarks in the DI is due to the fact that g_A^1 in the DI is large and negative, about $-0.12(1)$ for each

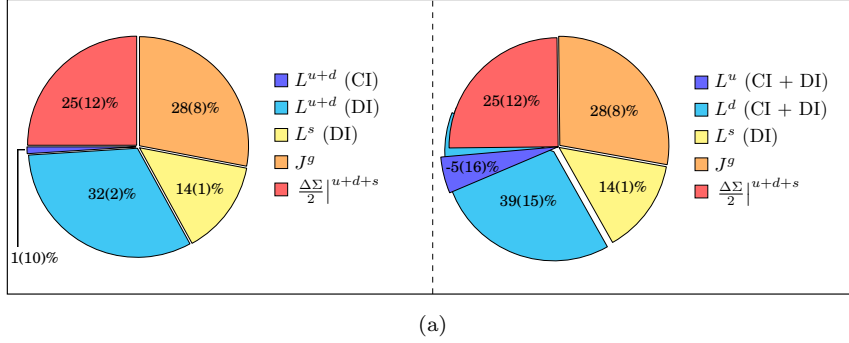


Fig. 4. Pie charts for the quark spin, quark orbital angular momentum and gluon angular momentum contributions to the proton spin. The left panel show the quark contributions separately for CI and DI, and the right panel shows the quark contributions for each flavor with CI and DI summed together for u and d quarks.

of the three flavors. All together, the quark OAM constitutes a fraction of 0.47(13) of the nucleon spin. The majority of it comes from the DI.

As far as the spin decomposition is concerned, it is found that the quark spin constitutes 25(12)% of the proton spin, the gluon total AM takes 28(8)% and the rest is due to the quark kinetic OAM which is 47(13)%.

Since this calculation is based on a quenched approximation which is known to contain uncontrolled systematic errors, it is essential to repeat this calculation with dynamical fermions of light quarks and large physical volume. However, we expect that the quark OAM fraction may still be large in the dynamical calculation.

In the naive constituent quark model, the proton spin comes entirely from the quark spin. On the other hand, in the Skyrme model⁶⁸ the proton spin originates solely from the OAM of the collective rotational motion of the pion field.⁶⁹ What is found in the present lattice calculation suggests that the QCD picture, aside from the gluon contribution, is somewhere in between these two models, indicating a large contribution of the quark OAM due to the meson cloud ($q\bar{q}$ pairs in the higher Fock space) in the nucleon.

5. Effective theory of baryons

Many estimates of quark spin and OAM contributions of the nucleon are based on quark models. However, quark models are not realistic effective theories of QCD, since they do not have chiral symmetry, a salient feature of

QCD whose dynamics governs light-quark hadron structure, spectroscopy, and scattering at low energies. It is being learned quantitatively through lattice calculations of quark spin from the anomalous Ward identity^{63,70,71} that the smallness of the quark spin contribution in the nucleon is related to the $U(1)$ anomaly, the same anomaly which is responsible for the large η' mass. This cannot be understood with quark models without the chiral $U(1)$ anomaly. Similarly, relativistic quark models do not explain the large OAM obtained from the lattice calculation in Sec. 4. Both the chiral quark model studies²⁶ and lattice calculation of valence QCD^{27,34} reveal that the level reversal of the positive and negative parity excited states of the nucleon, *i.e.* $P_{11}(1440)$ (Roper resonance) and $S_{11}(1535)$, and the hyperfine splittings between the decuplet and octet baryons are dominated by the meson-mediated flavor-spin interaction, not the gluon-mediated color-spin interaction. All of these point to the importance of the meson degree of freedom ($q\bar{q}$ pairs in the higher Fock space) which is missing in the quark model.

To see how this comes about, one can follow Wilson's renormalization group approach to effective theories. It is suggested by Liu *et al.*⁷² that the effective theory for baryons between the scale of $4\pi f_\pi$ ($\sim 1\text{GeV}$), which is the scale of the meson size ($l_M \sim 0.2\text{ fm}$), and $\sim 300\text{ MeV}$, which is the scale of a baryon size ($l_B \sim 0.6\text{ fm}$), should be a chiral quark model with renormalized couplings and renormalized meson, quark and gluon fields which preserve chiral symmetry. A schematic illustration for such division of scales^a for QCD effective theories is illustrated in Fig. 5.

This suggestion is based on the observation that mesons and baryon form factor assume a monopole and dipole form, respectively. Since the πNN form factor is much softer than the $\rho\pi\pi$ form factor, it is suggested that the confinement scale of quarks in the baryon l_B is larger than l_M – the confinement scale between the quark and antiquark in the meson. This is consistent with the large- N_c approach to hadrons where the mesons are treated as point-like fields and the baryons emerge as solitons with a size of order unity in N_c .⁷⁴ Taking l_M from the $\rho\pi\pi$ form factor gives $l_M \sim 0.2\text{ fm}$. This is very close to the chiral symmetry breaking scale set by $\Lambda_\chi = 4\pi f_\pi$. Considering them to be the same, operators of low-lying meson

^aWe should point out that although two scales are adopted here, they are distinct from those of Manohar and Georgi.⁷³ In the latter, the σ – quark model does not make a distinction between the quark fields in the baryons and mesons. As such, there is an ambiguity of double counting of mesons and $q\bar{q}$ states. By making the quark-quark confinement length scale l_B larger than the quark-antiquark confinement length scale l_M , one does not have this ambiguity.

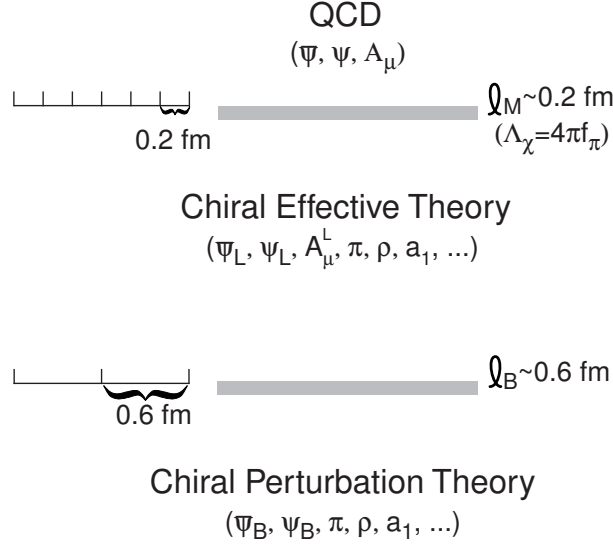


Fig. 5. A schematic illustration of the two-scale delineation of the effective theories. The shaded bars mark the positions of the cutoff scales l_M and l_B separating different effective theories.

fields become relevant operators below Λ_χ . As for the baryon confinement scale, Liu *et al.* take it to be the size characterizing the meson-baryon-baryon form factors. Defining the latter from the respective meson poles in the nucleon pseudoscalar, vector, and axial-vector form factors in a lattice calculation²⁷ (see Fig. 17 in the reference), they obtained $l_B \sim 0.6 - 0.7$ fm, satisfying $l_B > l_M$. Thus, in between these two scales l_M and l_B (corresponding to the scale of ~ 300 MeV), one could have coexistence of mesons and quarks in an effective theory for baryons.

An outline is given⁷² to show how to construct a chiral effective theory for baryons. In the intermediate length scale between l_M and l_B , one needs to separate the fermion and gauge fields into long-range ones and short-range ones

$$\psi = \psi_L + \psi_S, \quad A^\mu = A_L^\mu + A_S^\mu, \quad (10)$$

where ψ_L/ψ_S and A_L^μ/A_S^μ represent the infrared/ultraviolet part of the quark and gauge fields, respectively, with momentum components below/above $1/l_M$ or Λ_χ . One adds irrelevant higher-dimensional operators to the ordinary QCD Lagrangian with coupling between bilinear quark fields

and auxiliary fields as given in Ref.,⁷⁵ interpreting these quark fields as the short-range ones, *i.e.* ψ_S and $\bar{\psi}_S$. Following the procedure by Li in Ref.,⁷⁵ one can integrate out the short-range fields and perform the derivative expansion to bosonize ψ_S and $\bar{\psi}_S$. This leads to the Lagrangian with the following generic form:

$$\begin{aligned} \mathcal{L}_{\chi QCD} = & \mathcal{L}_{QCD'}(\bar{\psi}_L, \psi_L, A_L^\mu) + \mathcal{L}_M(\pi, \sigma, \rho, a_1, G, \dots) \\ & + \mathcal{L}_{\sigma q}(\bar{\psi}_L, \psi_L, \pi, \sigma, \rho, a_1, G, \dots). \end{aligned} \quad (11)$$

$\mathcal{L}_{QCD'}$ includes the original form of QCD but in terms of the quark fields $\bar{\psi}_L, \psi_L$, and the long-range gauge field A_L^μ with renormalized couplings. It also includes higher-order covariant derivatives.⁷⁶ \mathcal{L}_M is the meson effective Lagrangian, *e.g.* the one derived by Li⁷⁵ which should include the glueball field G . Finally, $\mathcal{L}_{\sigma q}$ gives the coupling between the $\bar{\psi}_L, \psi_L, G$ and mesons. As we see, in this intermediate scale, the quarks, gluons and mesons coexist and meson fields couple to the long-range quark fields. Going further down below the baryon confinement scale $1/l_B$, one can integrate out $\bar{\psi}_L, \psi_L$ and A_L^μ , resulting in an effective Lagrangian $\mathcal{L}(\bar{\Psi}_B, \Psi_B, \pi, \sigma, \rho, a_1, G, \dots)$ in terms of the baryon and meson fields.⁷⁷ This would correspond to an effective theory in the chiral perturbation theory. In order for the chiral symmetry to be preserved, the effective theory of baryons at the intermediate scale necessarily involves mesons in addition to the effective quark and gluon fields. This naturally leads to a chiral quark effective theory.

Models like the little bag model with skyrmion outside the MIT bag,⁷⁸ the cloudy bag model⁷⁹ and quark chiral soliton model⁸⁰ have the right degrees of freedom and, thus, could possibly delineate the pattern of division of the proton spin with large quark OAM contribution. In particular, the fact that the u and d OAM in the MIT bag and to some extent the LFCQM in Table 1 have different signs from those of the lattice calculation may well be due to the lack of meson contributions as demanded by chiral symmetry in the effective theory of baryons.

6. Summary

We discuss three examples in lattice QCD to highlight the role chiral symmetry and chiral dynamics play in baryons. From the observation of parity reversal of the excited the nucleon and Δ spectrum and the phenomenological model for the πN scattering and N^* states, it is suggested that it is the chiral dynamics that plays the leading role in the pattern of the low-lying baryon spectrum. This notion is supported by our study of the

valence QCD and the fact that the lattice calculation of the Roper state by the non-chiral fermions at relatively coarse lattice spacing are substantially higher (by several hundred MeV's) than that of the chiral fermion which agrees with experiment.

All the differences of lattice calculations with different fermion formulation are supposed to go away as the lattice spacing approaches zero due to universality. However, at finite lattice spacing, the different results from non-chiral and chiral fermions serve to illustrate the role of chiral symmetry and confirm the observation that chiral dynamic seems to be ubiquitous in low energy hadron physics. Thus, it is essential to incorporate Goldstone bosons in the effective theory of baryons in addition to quarks and gluons below the chiral scale of $4\pi f_\pi$.

7. In memoriam

This manuscript is dedicated to the memory of Gerald E. Brown who was the author's Ph. D. thesis advisor, a mentor in his professional career and a lifelong friend.

This work is supported partially by US Department of Energy grant de-sc0013065.

References

1. S. Weinberg, Phys. Rev. Lett. **17**, 616 (1966).
2. J. Gasser and H. Leutwyler, Nucl. Phys. **B250**, 465, 517, 539 (1985).
3. J. J. Sakurai, Phys. Rev. Lett. **17**, 1021 (1966); *Currents and Mesons*, 1969 (The University of Chicago Press).
4. K. Kawarabayashi and M. Suzuki, Phys. Rev. Lett. **16**, 255 (1966); Fayyazuddin and Riazuddin, Phys. Rev. **147**, 1071 (1966).
5. Y. Tomozawa, Nuovo Cim. **46A**, 707 (1966).
6. See, for example, M. Mattis in *Chiral Solitons*, ed. K.F. Liu (World Scientific, 1987), p. 171.
7. G. Adkins, C. R. Nappi, and E. Witten, Nucl. Phys. **228**, 552 (1983).
8. B. A. Li and K. F. Liu, *Chiral Solitons*, ed. K. F. Liu (World Publishing Co., 1987), p. 421.
9. M. Goldberger and S.B. Treiman, Phys. Rev. **110**, 1178 (1958).
10. G.E. Brown and J.D. Jackson, *The Nucleon-Nucleon Interaction*, North-Holland, 1976.
11. C.W. Wong and K.F. Liu, "Nucleon-Nucleon Interaction", Topics in Nuclear Physics, ed. T.T.S. Kuo and S.S.M. Wong, *Lecture Notes in Physics* **144**, 1-174 (Springer-Verlag 1981).
12. R. Vinh Mau, Lect. Notes Phys. **581**, 1 (2001); R. B. Wiringa, V. G. J. Stoks

- and R. Schiavilla, Phys. Rev. C **51**, 38 (1995), doi:10.1103/PhysRevC.51.38 [nucl-th/9408016]; R. Machleidt and I. Slaus, J. Phys. G: Nucl. Part. Phys. **27**, 69 (2001), [arXiv:nucl-th/0101056]; V. G. J. Stoks, R.A. M. Klomp, C. P. F. Terheggen and J.J. de Swart, Phys. Rev. C **49**, 2950 (1994), [arXiv:nucl-th/9406039].
13. G. E. Brown, Chiral symmetry and the nucleon-nucleon interaction, in: Mesons in Nuclei, Vol. 1, M. Rho and D. Wilkinson (eds.), North-Holland, Amsterdam (1979).
 14. D. O. Riska and G. E. Brown, Phys. Lett. B **38** (1972) 193.
 15. G. E. Brown and M. Rho, Phys. Lett. B **82** (1979) 177; G. E. Brown, A. D. Jackson, M. Rho and V. Vento, Phys. Lett. B **140** (1984) 285.
 16. G. E. Brown and M. Rho, Phys. Rev. Lett. **66** (1991) 2720.
 17. G. E. Brown and M. Rho, Phys. Rept. **363**, 85 (2002), [hep-ph/0103102].
 18. D. B. Kaplan, Phys. Lett. B **288**, 342 (1992), [hep-lat/9206013]; Y. Shamir, Nucl. Phys. **406**, 90 (1993), [hep-lat/9303005]
 19. H. Neuberger, Phys. Lett. B **417**, 141 (1998).
 20. K. F. Liu, Nucl. Phys. A **928**, 99 (2014), [arXiv:1404.3754 [hep-ph]].
 21. See, e.g. S. Capstick and W. Roberts, Prog. Part. Nucl. Phys. **45**, S241 (2000), [nucl-th/0008028].
 22. K.F. Liu and C.W. Wong, Phys. Rev. **D28**, 170 (1983).
 23. S. Capstick and N. Isgur, Phys. Rev. **D34**, 2809 (1986).
 24. K.F. Liu, J.S. Zhang, and G.R.E. Black, Phys. Rev. **D30**, 2015 (1984); J. Breit and C.R. Nappi, Phys. Rev. Lett. **53**, 889 (1984).
 25. U.B. Kaulfuss and U-G. Meissner, Phys. Lett. **154B**, 193 (1985).
 26. L.Y. Glozman and D.O. Riska, Phys. Rep. **268**, 263 (1996).
 27. K.F. Liu, S.J. Dong, T. Draper, D. Leinweber, J. Sloan, W. Wilcox, R. Woloshyn, Phys. Rev. **D59** 112001 (1999).
 28. T. Barnes and F.E. Close, Phys. Lett. **123B**, 221 (1983); Z. Li, Phys. Rev. **D44**, 2841 (1991); C.E. Carlson and N.C. Mukhopadhyay, Phys. Rev. Lett. **67**, 3745 (1991).
 29. O. Krehl, C. Hanhart, S. Krewald, J. Speth, Nucl. Phys. **C62**, 025207 (2000); R. Jaffe and F. Wilczek, Eur. Phys. J. C **33**, S38 (2004).
 30. M. Mahbub, W. Kamleh, D.B. Leinweber, P. Moran, and A.G. Williams, Phys. Lett. **B707**, 389 (2012), [arXiv:1011.5724].
 31. R.G. Edwards, J.J. Dudek, D.G. Richards, and S.J. Wallace, Phys. Rev. **D84**, 074508 (2011), [arXiv:1104.5152].
 32. C. Alexandrou, T. Leontiou, C. N. Papanicolas and E. Stiliaris, Phys. Rev. D **91** (2015) no.1, 014506, [arXiv:1411.6765 [hep-lat]].
 33. G. P. Engel, C. Lang, D. Mohler, and A. Schfer (BGR), Phys.Rev. **D87**, 074504 (2013), 1301.4318.
 34. K. F. Liu, Y. Chen, M. Gong, R. Sufian, M. Sun and A. Li, PoS LATTICE **2013**, 507 (2014), [arXiv:1403.6847 [hep-ph]].
 35. N. Mathur, Y. Chen, S.J. Dong, T. Draper, I. Horváth, F.X. Lee, K.F. Liu, and J.B. Zhang, Phys. Lett. **B605**, 137 (2005), [arXiv:hep-ph/0306199].
 36. B. G. Lasscock, J. N. Hedditch, W. Kamleh, D. B. Leinweber, W. Melnitchouk, A. G. Williams, J. M. Zanotti, Phys. Rev. **D76**, 054510 (2007).

37. Y. Chen *et al.*, hep-lat/0405001.
38. B. Julia-Diaz, H. Kamano, T. -S. H. Lee, A. Matsuyama, T. Sato and N. Suzuki, Phys. Rev. C **80**, 025207 (2009), [arXiv:0904.1918 [nucl-th]].
39. N. Suzuki, B. Julia-Diaz, H. Kamano, T. -S. H. Lee, A. Matsuyama and T. Sato, Phys. Rev. Lett. **104**, 042302 (2010), [arXiv:0909.1356 [nucl-th]].
40. R. D. Young and A. W. Thomas, Phys. Rev. D **81** (2010) 014503, [arXiv:0901.3310 [hep-lat]].
41. G. S. Bali *et al.* [RQCD Collaboration], Phys. Rev. D **93**, no. 9, 094504 (2016), [arXiv:1603.00827 [hep-lat]].
42. L. S. Brown, W. J. Pardee and R. D. Peccei, Phys. Rev. D **4**, 2801 (1971).
43. T. P. Cheng and R. F. Dashen, Phys. Rev. D **4**, 1561 (1971).
44. D. B. Kaplan and A. E. Nelson, Phys. Lett. B **175**, 57 (1986).
45. M. A. Shifman, A. I. Vainshtein and V. I. Zakharov, Phys. Lett. B **78**, 443 (1978).
46. M. Gong *et al.* [XQCD Collaboration], Phys. Rev. D **88**, 014503 (2013), doi:10.1103/PhysRevD.88.014503 [arXiv:1304.1194 [hep-ph]].
47. T. Falk, A. Ferstl and K. A. Olive, Phys. Rev. D **59**, 055009 (1999) [Phys. Rev. D **60**, 119904 (1999)] [hep-ph/9806413].
48. J. R. Ellis, K. A. Olive and C. Savage, Phys. Rev. D **77**, 065026 (2008), [arXiv:0801.3656 [hep-ph]].
49. J. Giedt, A. W. Thomas and R. D. Young, Phys. Rev. Lett. **103**, 201802 (2009), [arXiv:0907.4177 [hep-ph]].
50. J. Gasser, H. Leutwyler and M. E. Sainio, Phys. Lett. B **253**, 252 (1991).
51. T. Becher and H. Leutwyler, Eur. Phys. J. C **9**, 643 (1999), [hep-ph/9901384].
52. M. M. Pavan, I. I. Strakovsky, R. L. Workman and R. A. Arndt, PiN Newslett. **16**, 110 (2002), [hep-ph/0111066].
53. J. M. Alarcon, J. Martin Camalich and J. A. Oller, Phys. Rev. D **85**, 051503 (2012), [arXiv:1110.3797 [hep-ph]].
54. Y. H. Chen, D. L. Yao and H. Q. Zheng, Phys. Rev. D **87**, 054019 (2013), [arXiv:1212.1893 [hep-ph]].
55. M. Hoferichter, J. Ruiz de Elvira, B. Kubis and U. G. Meiner, Phys. Rev. Lett. **115**, 092301 (2015), doi:10.1103/PhysRevLett.115.092301, [arXiv:1506.04142 [hep-ph]].
56. C. Michael *et al.* [UKQCD Collaboration], Nucl. Phys. Proc. Suppl. **106**, 293 (2002), doi:10.1016/S0920-5632(01)01692-9, [hep-lat/0109028].
57. K. Takeda *et al.* [JLQCD Collaboration], Phys. Rev. D **83**, 114506 (2011) doi:10.1103/PhysRevD.83.114506 [arXiv:1011.1964 [hep-lat]].
58. G. S. Bali *et al.* [QCDSF Collaboration], Phys. Rev. D **85**, 054502 (2012), doi:10.1103/PhysRevD.85.054502, [arXiv:1111.1600 [hep-lat]]; G. S. Bali *et al.* [RQCD Collaboration], Phys. Rev. D **93**, no. 9, 094504 (2016) doi:10.1103/PhysRevD.93.094504 [arXiv:1603.00827 [hep-lat]].
59. Y. B. Yang, A. Alexandru, T. Draper, J. Liang and K. F. Liu, arXiv:1511.09089 [hep-lat].
60. D. de Florian, R. Sassot, M. Stratmann and W. Vogelsang, Phys. Rev. D **80**, 034030 (2009) [arXiv:0904.3821 [hep-ph]].
61. P. Hasenfratz, V. Laliena and F. Niedermayer, Phys. Lett. B **427**, 125 (1998),

- doi:10.1016/S0370-2693(98)00315-3, [hep-lat/9801021].
62. Y. Kikukawa and A. Yamada, Phys. Lett. B **448**, 265 (1999) [hep-lat/9806013]; D. H. Adams, Annals Phys. **296**, 131 (2002) [hep-lat/9812003]; K. Fujikawa, Nucl. Phys. B **546**, 480 (1999) [hep-th/9811235]; H. Suzuki, Prog. Theor. Phys. **102**, 141 (1999) [hep-th/9812019].
 63. M. Gong, Y. B. Yang, A. Alexandru, T. Draper and K. F. Liu, arXiv:1511.03671 [hep-ph].
 64. E. Leader and C. Lorc, Phys. Rept. **541**, 163 (2014), doi:10.1016/j.physrep.2014.02.010 [arXiv:1309.4235 [hep-ph]].
 65. K. F. Liu and C. Lorc, Eur. Phys. J. A **52**, no. 6, 160 (2016), doi:10.1140/epja/i2016-16160-8, [arXiv:1508.00911 [hep-ph]].
 66. X. D. Ji, Phys. Rev. Lett. **78**, 610 (1997), [hep-ph/9603249].
 67. M. Deka *et al.*, Phys. Rev. D **91**, no. 1, 014505 (2015), doi:10.1103/PhysRevD.91.014505, [arXiv:1312.4816 [hep-lat]].
 68. G. S. Adkins, C. R. Nappi and E. Witten, Nucl. Phys. B **228**, 552 (1983).
 69. B.A. Li, AIP Conf.Proc. **343** (1995) 802-806, DOI: 10.1063/1.48961.
 70. Y. B. Yang, M. Gong, K. F. Liu and M. Sun, PoS LATTICE **2014**, (2014) 138.
 71. K. F. Liu, Int. J. Mod. Phys. Conf. Ser. **40**, 1660005 (2016) doi:10.1142/S2010194516600053 [arXiv:1504.06601 [hep-ph]].
 72. K. F. Liu, S. J. Dong, T. Draper, J. H. Sloan, W. Wilcox and R. M. Woloshyn, Phys. Rev. D **61**, (2000) 118502.
 73. A. Manohar and H. Georgi, Nucl. Phys. B **234**, (1984) 189.
 74. E. Witten, Nucl. Phys. **B160**, 57 (1979).
 75. B. A. Li, Phys. Rev. D **52**, 5165 (1995), [hep-ph/9504304].
 76. B. J. Warr, Annals Phys. **183**, 1 (1988).
 77. Q. Wang, Y. P. Kuang, X. L. Wang and M. Xiao, hep-ph/9910289.
 78. G. E. Brown and M. Rho, Phys. Lett. B **82**, 177 (1979).
 79. A. W. Thomas, S. Theberge and G. A. Miller, Phys. Rev. D **24**, 216 (1981).
 80. M. Wakamatsu and Y. Nakakoji, Phys. Rev. D **74**, 054006 (2006).